Proceedings of ERAD (2004): 162–167 © Copernicus GmbH 2004

ERAD 2004

Revisiting the latent heat nudging scheme for the rainfall assimilation in convective systems

D. Leuenberger and A. Rossa

MeteoSwiss, Krähbühlstrasse 58, 8044 Zürich, Switzerland

Abstract. Next-generation, high-resolution numerical weather prediction models require accurate and economical assimilation schemes for radar data. In this study, we reevaluate the Latent Heat Nudging (LHN) scheme, a simple assimilation scheme for rainfall data, within a meso-γ NWP model by means of experiments with simulated and radar-derived rainfall observations. The idealised tests indicate that the LHN scheme is well able to capture the dynamical structure and the right rainfall amount of a simulated supercell storm in a perfect environment. Even in degraded environments, the scheme is able to assimilate the storm, but the rainfall amount and distribution can vary considerably. Errors in the humidity field primarily impact the precipitation amount in the assimilation cycle, whereas changes in the wind field can cause interferences between the LHN scheme and the storm dynamics leading to a distorted dynamical structure and rainfall distribution of the assimilated storm. The scheme is quite sensitive to errors in the observations, where position and structure errors are found to be more serious than amplitude errors. A case study of severe convection confirms the potential of rainfall assimilation in reducing the spin-up in the forecast. The information provided by the radar has a beneficial impact in the prediction of precipitation over the entire lifetime of the convective system.

1 Introduction

Short-range numerical weather prediction (NWP) depends on a proper definition of the initial model state and, particularly when aiming at quantitative precipitation forecasting, the hydrological cycle, in order to reduce the spin-up in the forecast. Since weather radars offer high-resolution observations of precipitation related phenomena they become an increasingly important complement to conventional observations for assimilation into and verification of NWP models, issues that are pursued in the COST-717 action "'On the Use of Radar Information in Hydrological and NWP Models" (Rossa, 2000).

Correspondence to: D. Leuenberger
(daniel.leuenberger@meteoswiss.ch)

Rainfall assimilation is a long standing problem and has received much attention in the past (see Alberoni et al., 2003; Park and Zupanski, 2003, for a review). On the mesoscale and storm-scale radar-derived rain is increasingly used in the analysis (e.g. Jones and Macpherson, 1997; Sun and Crook, 1997; Ducrocq et al., 2002; Haase et al., 2000). Overall, the assimilation of rainfall data has shown considerable potential to reduce the spin-up effect and the development of suitable schemes is still an active research field. Currently, four dimensional variational (4DVAR) and Ensemble Kalman Filter (EnKF) methods are being tested on the mesoscale and storm-scale using simulated and real Doppler radar winds and reflectivity data (e.g. Sun and Crook, 1997; Snyder and Zhang, 2003). These methods are computationally very expensive. Next generation NWP systems will have mesh sizes of O(1 km) and sophisticated microphysical parametrisations in order to cope with the explicit simulation of convection. It is therefore important to reevaluate and develop computationally efficient schemes for the operational assimilation of high-frequency, rain-related observations.

Latent Heat Nudging (LHN) is a simple and economical method for the assimilation of surface rain and has come to successful operational application in large-scale and mesoscale NWP systems (Jones and Macpherson, 1997; Lin et al., 2001).

The present study tries to make a contribution to the reevaluation and characterisation of the LHN at the storm-scale by means of experiments with simulated and radar-derived surface rainfall observations. Consideration is given to the dynamical forcing of convective storms and to the sensitivity of the LHN scheme to observation frequency and errors in the environment and in the rainfall data.

Table 1. List of idealised assimilation experiments with simulated observations. In the third column, the 3h area total precipitation at the end of each experiment (in 10^6 m^3) is listed.

Name	Description	Rain
REF	Reference simulation	12.2
CNTL	Identical twin experiment	12.8
IF1A	Obs. insertion frequency of 6 min	22.0
IF2A	Obs. insertion frequency of 10 min	34.6
O1A	Error in observations (factor 0.5)	11.2
O2A	Error in observations (factor 2)	17.1
H1A	Error in PBL humidity (r = 11.5 g/kg)	11.0
H2A	Error in PBL humidity (r = 12.5 g/kg)	14.2
H3A	Error in PBL humidity (r = 13.0 g/kg)	16.5
W1A	Error in wind (- 2 m/s)	16.2
W2A	Error in wind (+ 2 m/s)	14.4

2 Methodology

2.1 Model

The model used in this study is the non-hydrostatic, fully compressible Local Model (LM). Prognostic variables include the three Cartesian velocity components (u, v and w), temperature (T), pressure perturbation (p') and mass fractions of water vapour (q_v) and cloud water (q_c). The parametrisation for grid-scale precipitation accounts for four categories of water (water vapour, cloud water, rain and snow). A detailed description of the model is given by Steppeler et al. (2003).

2.2 Assimilation Scheme

The main principle of the LHN is to correct the model's latent heating (LH) at each time step by a factor derived from the ratio of observed and model-estimated surface precipitation. The vertical shape of the forcing is given by the model LH based on the assumption that its distribution is sensible. If there are large discrepancies between observed and modelled rain rates, the scaling factor is limited (to a factor of 2 in this study, i.e. the model profiles are at most doubled/halved) so that there is not too much heat added to or removed from the model. More details on the scheme can be found in Jones and Macpherson (1997) and Leuenberger and Rossa (2003).

3 Idealised Studies

A series of assimilation experiments (see Table 1 for a listing) with simulated rain fields from an idealised supercell type storm are performed in order to test the LHN scheme in a simple environment and on a long-lived, coherent convective system of known structure and evolution.

3.1 Setup of Experiments and Reference Simulation

The computational domain consists of 250×100 km with a mesh size of 1 km and a stretched vertical grid with 60 levels. Neither soil nor radiative forcings are considered, the convection parametrisation scheme is switched off and Coriolis effects are neglected. All simulations are integrated 180 min with a time step of 5 s.

The environment of the reference simulation is chosen to be supportive for splitting supercell storms and constructed following Weisman and Klemp (1982). It is characterised by a moist, well mixed boundary layer with a constant water vapour mixing ratio of 12 g/kg, and a large amount of CAPE (1200 J/kg). The environmental wind exhibits a unidirectional vertical shear of 20 m/s over the lowest 4 km.

The convective system of the reference simulation is triggered with a warm bubble in the western part of the domain. It first develops as a single cumulus and gradually splits into two counterrotating updrafts (transition stage). After t=50 min the two storms move quasi-steadily in northwest (south-east) direction (posttransition stage). Figure 1a shows the 3 h cumulated surface rainfall at the end of the simulation (only the right part of the storm is depicted, since the left part is a mirror image of it). The 3 h total cumulated rain is $12.8 \cdot 10^6$ m^3 (see Table 1). A vertical cross-section of the storm at t=100 min (Fig. 1b) reveals the deep cloud system with a leading anvil and the distinct heavy precipitation zone topped by a strong updraft region and a horizontal cross-section shows the corresponding vorticity and moisture convergence at the outflow boundary (Fig. 1c).

The reference run serves as 'truth' against which the assimilation experiments are quantitatively compared. Root mean square errors (RMSE) of selected model fields are calculated in a moving frame of 25×25 gridpoints around the storm and over the whole depth of the domain. Figure 2 presents results for the vertical velocity, but the scores for other fields (as horizontal velocity or temperature) are qualitatively similar.

3.2 Assimilation Simulation

For the test of the LHN scheme an identical twin experiment (CNTL) is performed, where the environment and the model are the same as in the reference simulation (i.e. assumed perfect), but no triggering warm bubble is added. The pseudo rainfall observations for the assimilation are extracted from the reference run every minute. In this setup the LHN scheme is well able to assimilate the storm. Not only the 3 h precipitation amount (5% deviation from the reference run) and the rainfall distribution (Fig. 1d), but also the dynamical structure at t=100 min (Fig. 1e,f) is well reproduced and the nudging temperature increment is small during the posttransition stage. The RMSE of w (Fig. 2, thick black line) saturates after roughly 60 min, i.e. after the transition stage of the reference storm.

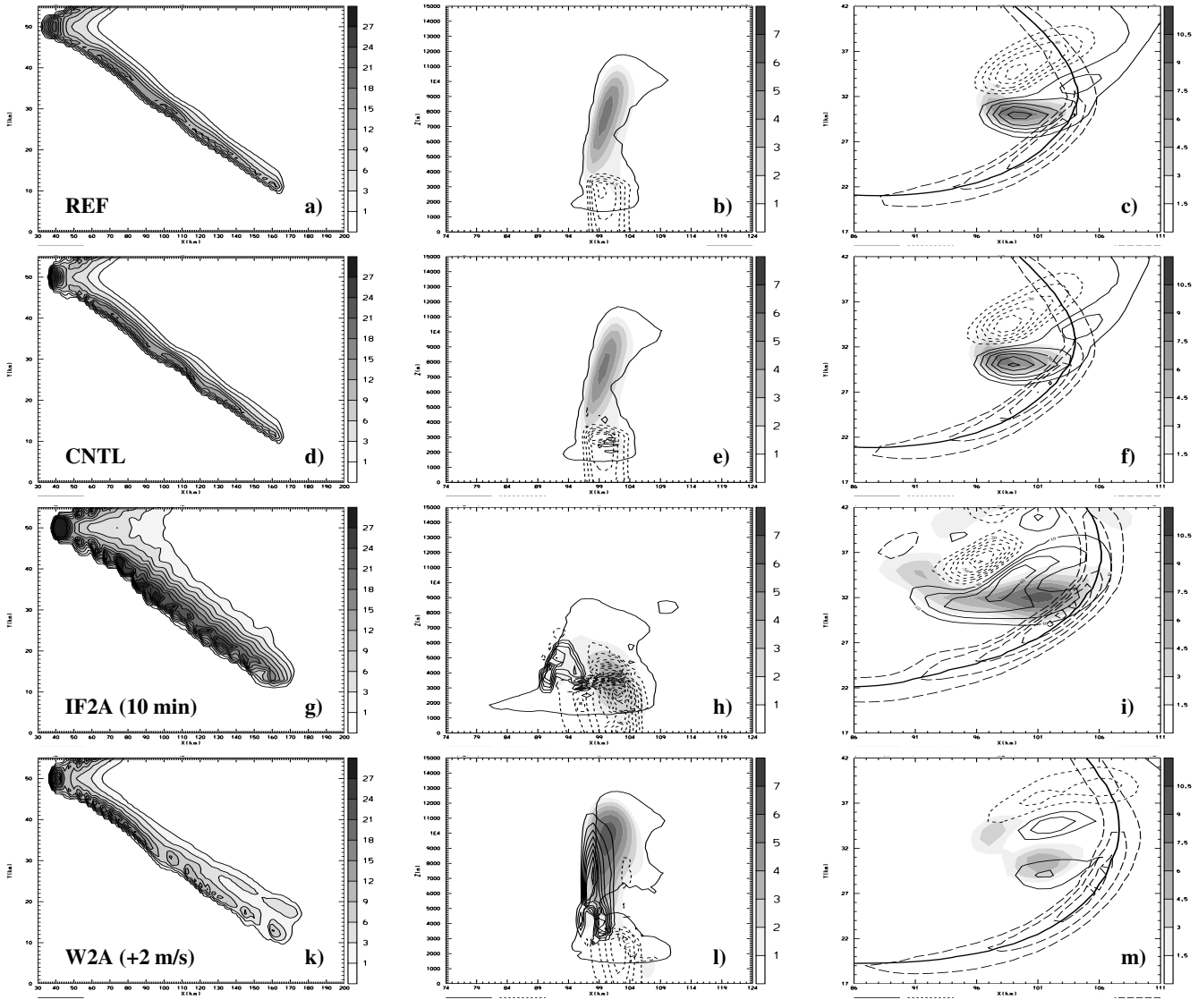

Fig. 1. Selected results from the idealised experiments (see Table 1 for a description). Left panels: 3 h cumulated surface precipitation (in mm) valid at 180 min. Middle panels: vertical cross-sections (averaged over 10 grid points) of vertical velocity w (in m/s, shaded, only positive values are plotted), nudging temperature increment (0.0015 K/s contour interval, thin solid lines for positive values, thin dashed lines for negative values), cloud water q_c (0.1 g/kg contour, thick solid line) and rain water q_r (0.5 g/kg contour interval, thick dashed lines) valid at 100 min. Right panels: w (in m/s, shaded) and vertical vorticity ($10 \cdot 10^{-4}\ s^{-1}$ contour interval , thin solid lines for positive values, thin dashed lines for negative values) at $z = 4000$ m, moisture divergence at $z = 50$ m ($2 \cdot 10^{-5}\ s^{-1}$ contour interval, thick dashed contours, only negative values are plotted), and -0.5 K contour of surface perturbation temperature (thick solid contour) valid at 100 min.

3.3 Sensitivity Studies

Since in real applications neither a perfect model nor a perfect environment is available, the performance of the LHN scheme under non-perfect conditions is evaluated. Experiments are carried out where the rainfall observations are degraded or the storm environment is altered.

3.3.1 Degraded Observations

First, the sensitivity of the LHN scheme to the temporal resolution of the observations is investigated. This is accomplished by decreasing the sampling frequency of the pseudo observation extraction to 6 min (for exp. IF1A) and 10 min (for exp. IF2A). Typical radar systems provide observations every 5 to 15 min. As the LHN scheme interpolates the observations linearly between two subsequent observing times the area of the assimilated signal increases with increasing time intervals, i.e. smaller insertion frequency. This artefact yields an amplitude error and an areal mismatch that can be regarded as a position error. The resulting effect on the storm assimilation is negative and can be quite serious. The enlarged forcing area causes a 3h rainfall increase of 71% (170%) for an insertion frequency of 6 min (10 min) compared to the CNTL run. This is also apparent

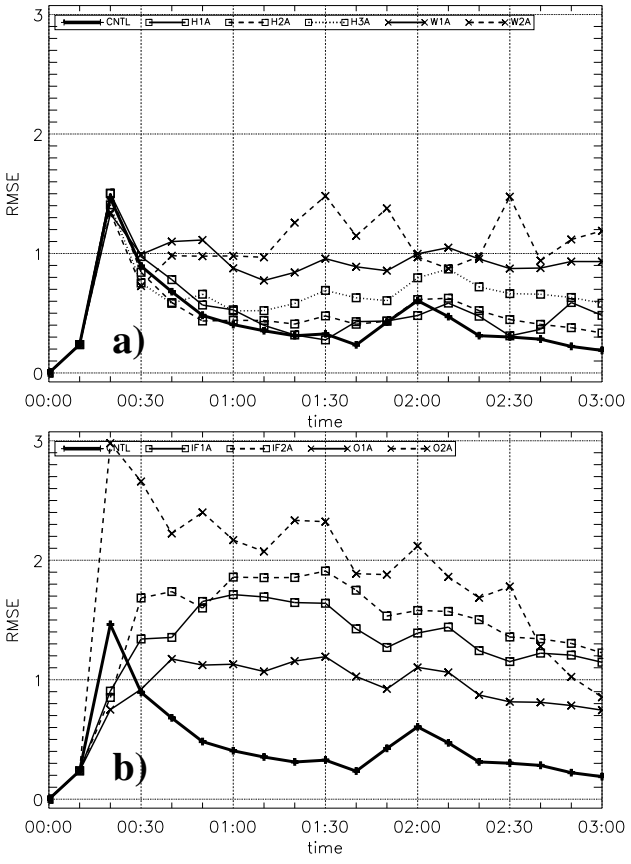

Fig. 2. Time series of vertical velocity root mean square errors (in m/s) for the idealised experiments compared against the reference simulation. Panel a): experiments with degraded environment, panel b): experiments with degraded observations.

in the distribution of the 3h rain field of experiment IF2A (Fig. 1g). The dynamical structure of the storm is highly degraded and widespread temperature assimilation increments (Fig. 1h) and a large updraft area (Fig. 1i) are apparent. The RMSE errors of w are three to four times as large as those of the CNTL experiment (Fig. 2b).

In order to simulate the effect of observation amplitude errors, two assimilation experiments are made where the pseudo observations are multiplied by a factor of 0.5 (underestimation, exp. O1A) and 2.0 (overestimation, exp. O2A). These factors can be taken as a very rough estimate of the radar rainfall accuracy over well covered terrain. The cumulated rain of the assimilated storms is not halved (doubled), as could be expected, but amounts to 88% (133%) of the CNTL experiment. The shape of the rainfall distribution does not differ much from that of the CNTL experiment, but the vertical storm extent, updrafts and assimilation temperature increments are reduced (enhanced) (not shown). This is reflected in the RMSE of the vertical velocity, which reveals significantly larger errors for the case of overestimation when compared to the case of underestimation.

The sensitivity of the LHN scheme to non-rain echos is investigated in a series of experiments with simulated and real spurious rainfall signals. Results indicate that even a 1×1 pixel observation can trigger convection when constantly forced by the LHN scheme. In addition, the instability can be released very rapidly e.g. after 3 (8,20,50) minutes for an echo amplitude of 60 (20,10,5) mm/h. The amplification of the rain through the model is sensitive to the available CAPE. Although 98% of the ground clutter is removed in the preprocessing of the Swiss Radar Network remaining non-rain echos can be drastically amplified when assimilated into an unstable environment. Anaprop contaminated radar data appears not to be a serious problem because of the stable atmosphere (strong inversion) usually connected to this phenomenon.

3.3.2 Degraded Environment

One of the major difficulties in storm-scale analysis is the representation of the mesoscale environment into which the convective system is to be assimilated. In this section we present a number of assimilation experiments where the environment is degraded by changing the boundary layer humidity or the ambient wind. Observations are available as in the CNTL run.

The amount and distribution of atmospheric humidity is crucial in the precipitation building process, but is poorly represented in today's NWP systems. Typical mean errors in relative humidity compared against radiosondes reach values up to 10% but can be considerably larger in single cases. Park (1999) found that simulated supercells are very sensitive to low level humidity: even small changes lead to different storm development. Three experiments are carried out to test the sensitivity of the assimilated storms to changes in the boundary layer humidity. The mixing ratio of water vapour (r) is set to values of 11.5 g/kg (experiment H1A), 12.5 g/kg (exp. H2A) and 13 g/kg (exp. H3A). These values reflect errors in the mixing ratio of -4%, +4% and 8% respectively. A value of 11 g/kg is not enough for the evolution of a long lived storm (in agreement with the findings of Weisman and Klemp (1982)) and is not considered therefore. The LHN scheme is able to assimilate the storm into the different environments, but deviations of the rainfall amount -14% for experiment H1A, 11% for exp. H2A and 29% for exp. H3A, compared to the CNTL. In the drier (moister) environment the assimilation scheme needs to generate stronger (weaker) updrafts to produce the same amount of rain. The RMSE of the experiments with ±4% humidity error increase by about 30–40% on average, while a 8% humidity error causes roughly a doubled RMSE as compared to the CNTL.

The ambient wind field is another key variable determining the evolution of convective systems. A constant bias of -2 m/s (experiment W1A) and $+2$ m/s (experiment W2A) is added to the wind field of the assimilation environment. The rainfall forcing propagation velocity is therefore higher (lower) compared to the propagation velocity determined by the environmental wind of experiment W1A (W2A) and the resulting phase shift between the observations and the storm can be interpreted as a constant observation position error.

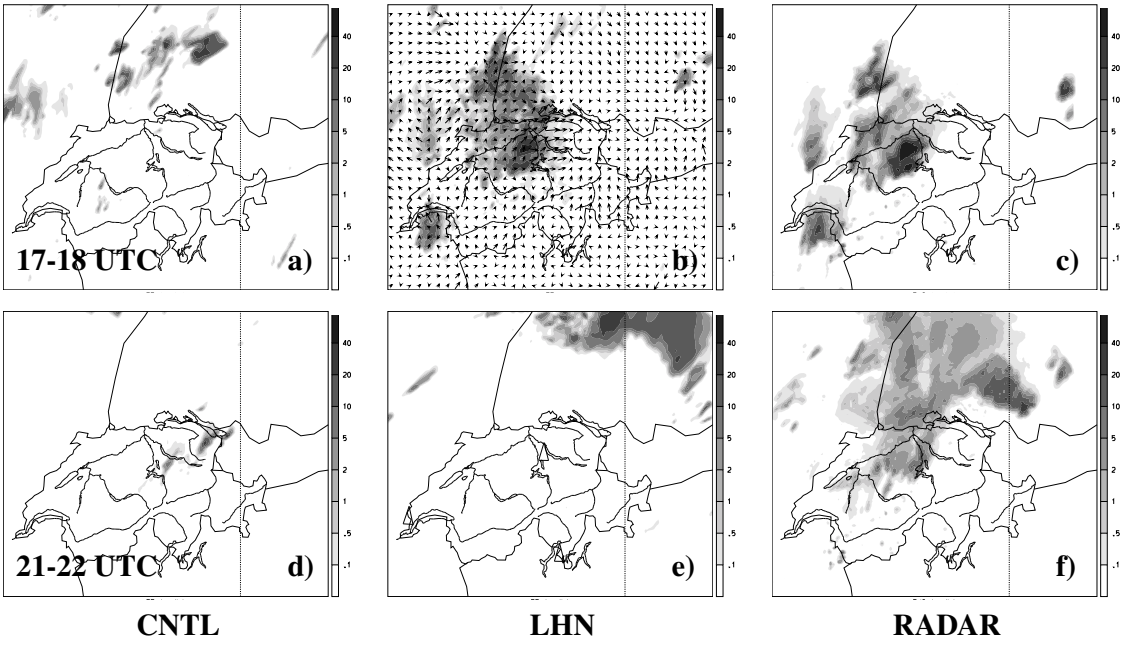

Fig. 3. Results from the 8 May 2004 case study. Displayed are hourly sums of precipitation (in mm, shaded) at 17–18 UTC (upper panels) and 21–22 UTC (lower panels). Left panels show results from the CNTL run (without radar assimilation), middle panels from the LHN run (radar assimilation from 12–18 UTC) and right panels show radar-derived rainfall. The 10 m wind field (arrows every 6 grid point, maximum of 12 m/s) valid at 18 UTC is overlayed on panel b). The location of the three Swiss radar stations is marked with triangles on panel e)

If the forcing moves faster than the storm new updrafts are forced ahead of the system, thus enlarging the updraft area in phase with the propagation. Rainfall distribution and structure of the system are similar to that of the CNTL experiment (not shown), but the enlarged updraft area results in the 3h rainfall to be 26% higher. The RMSE is three times as large as that of the CNTL run, partly due to phase errors.

The slower moving forcing, on the other hand, causes the LHN to cool (heat) ahead of (behind) the system (Fig. 1l) thus decelerating the storm. As this is against the movement of the system dynamical interferences between the forcing and the model storm dynamics cause a distorted evolution of the assimilated supercell. Particularly, the surface outflow boundary is gradually decoupled from the updraft and the low-level moisture supply is cut off (Fig. 1m), yielding a gradually decreasing rainfall intensity (Fig. 1k). These effects combine to lift the level of the LH to drier regions and increase the vertical velocity without producing the required rain intensity and consequently distort the dynamical fields in this region. The interferences are also reflected in a high RMSE.

4 Case Study of 8 May 2003

In this section we present an LHN assimilation experiment of a case of severe convection, that was well observed by the operational Swiss Radar Network (SRN). The synoptic situation of 8 May 2003 12 UTC is characterised by an upper-level trough over Spain. A weak cold front is located just west of Switzerland. At 16 UTC a multicell type storm develops over the Swiss Plateau. Due to a strong environmental wind shear the main cell exhibits supercell characteristics (rotation and movement right to the mean wind).

4.1 Radar Data

The Swiss Radar Network consists of three C-band Doppler Radars (see Fig. 3e for their locations), providing corrected (e.g. clutter elimination and vertical profile correction algorithms) surface rain rates every five minutes. A description of the radar system can be found in Joss et al. (1998). The rain rates are interpolated to the model grid for the assimilation.

4.2 Numerical Experiments

High-resolution numerical simulations with a mesh size of 2.2 km are carried out on a roughly 800×730 km large domain centered over Switzerland. Initial and hourly boundary conditions are provided from a 7 km LM forecast driven by ECMWF analyses and full physical parametrisations are used with the exception of the cumulus parametrisation scheme. Two 12h simulations starting at 8 May 2003, 12 UTC are performed, one without rainfall assimilation (CNTL) and one where radar data is inserted from 12 UTC to 18 UTC, followed by a 6h free forecast.

At 18 UTC the storm has fully developed and the main cell is located over the central part of the Swiss Plateau as visible from 1h cumulated radar-derived rainfall (Fig. 3c). The CNTL simulation does not capture the main storm but a few cells are placed north of Switzerland (Fig. 3a). The radar assimilation is able to trigger the convection at the

right location and approximatively with the right amount, high amplitudes being slightly underestimated and low amplitudes slightly overestimated (Fig. 3b). Four hours later the convective system has moved northeast and lost strength, while over central Switzerland new convection is observed (Fig. 3f). The CNTL run shows some weak rain patterns over the eastern part of the domain (Fig. 3d) but has not developed the main system. The 4h free forecast started from the radar analysis at 18 UTC still shows the convective system, but located too far to the northeast (Fig. 3e). Indeed, the system persists in the model for six hours in this case, as confirmed by an additional experiment, where the forcing is switched off at 14 UTC (not shown). This indicates that the environmental instability is appropriate for this case.

A possible reason for the position error in the forecast is that the outflow of the assimilated storm is located at the stratiform boundaries of the observed precipitation, some 50 km downstream of the main updraft (Fig. 3b), as the LHN scheme does not discern between convective and stratiform rain areas. Hence, new convection is triggered too far downstream of the main cell leading to the position error in the subsequent forecast. Furthermore, if the outflow boundary is decoupled from the main updraft the moisture supply for the rotating cell can be cut off, causing its rapid dissipation (similarly to the mechanism described in Sect. 3.3.2). Convective cells are often surrounded by stratiform rain areas, which are not driven by buoyancy, but rather by advection of precipitation (Houze, 1993). Therefore, stratiform regions should not be subject to buoyancy enhancement by the LHN scheme but should be formed by the model dynamics.

5 Conclusions

In this study, an attempt was made to characterise the LHN scheme within a meso-γ NWP model by means of experiments with simulated and radar-derived rainfall observations. The idealised tests indicate that the LHN scheme is well able to reproduce the dynamical structure as well as the right rainfall amount of a simulated supercell storm in a perfect environment. Even in degraded environments, the scheme is able to assimilate the storm, but the rainfall amount and distribution can vary considerably. Errors in humidity primarily cause changes in the assimilated precipitation amount, where changes in the wind field can cause interferences between the LHN scheme and the storm dynamics leading to a distorted dynamical structure and rainfall distribution of the assimilated storm. The scheme is quite sensitive to errors in the observations, where position and the structure errors are more serious than amplitude errors.

In a case of severe convection over the Swiss Plateau the LHN scheme performs well in that it successfully introduces the system in the right place and about the correct intensity. During the subsequent forecast the system persists in the simulation but exhibits a position error. Overall the impact of the radar assimilation on the precipitation forecast is beneficial over the entire lifetime of the convective system.

The LHN scheme forces rainfall via introducing buoyancy and is, therefore, not suitable for handling stratiform regions in a convective system. Experiments are underway to restrict the LHN to convective regions.

References

Alberoni, P. P., Ducrocq, V., Gregoric, G., Haase, G., Hollemann, I., Lindskog, M., Macpherson, B., Nuret, M., and Rossa, A.: Quality and assimilation of radar data for NWP – A Review, COST-717 report, 2003.

Ducrocq, V., Ricard, D., Lafore, J.-P., and Orain, F.: Storm-scale Numerical Rainfall Prediction for Five Precipitating Events over France: On the Importance of the Initial Humidity Field, Weather and Forecasting, 17, 1236–1256, 2002.

Haase, G., Crewell, S., Simmer, C., and Wergen, W.: Assimilation of radar data in mesoscale models: Physical initialization and latent heat nudging, Phys. Chem. Earth (B), 25, 1237–1242, 2000.

Houze, R.: Cloud Dynamics, Academic Press, New York, pp. 573, 1993.

Jones, C. D. and Macpherson, B.: A Latent Heat Nudging Scheme for the Assimilation of Precipitation Data into an Operational Mesoscale Model, Meteorol. Appl., 4, 269–277, 1997.

Joss, J., Schädler, B., Galli, G., Cavalli, R., Boscacci, M., Held, E., della Bruna, G., Kappenberger, G., Nespor, V., and Spiess, R.: Operational Use of Radar for Precipitation Measuerments in Switzerland, Tech. rep., Final Report, NRP 31, vdf Hochschulverlag an der ETH Zuerich, 108 pp., ISBN 3 7281 2501 6, http://vdf.ethz.ch, 1998.

Leuenberger, D. and Rossa, A.: Assimilation of Radar Information in aLMo, COSMO Newsletter, No. 3, available from http://www.cosmo-model.org, 2003.

Lin, Y., Baldwin, M. E., Mitchell, K. E., Rogers, E., and DiMego, G. J.: Spring 2001 Changes to NCEP ETA Analysis and Forecast System: Assimilation of Observed Precipitation Data, in Preprints, 18th Conference on Weather Analysis and Forecasting, Ft. Lauderdale, Florida, p. 4, 2001.

Park, S. K.: Nonlinearity and Predictability of Convective Rainfall associated with Water Vapour Perturbations in a Numerically Simulated Storm, Journal of Geophysical Research (Atmospheres), 104, 31 575–31 587, 1999.

Park, S. K. and Zupanski, D.: Four-Dimensional Variational Data Assimilation for Mesoscale and Storm-Scale Applications, Meteorol. Atmos. Phys., 82, 173–208, 2003.

Rossa, A.: COST-717: Use of Radar Observations in Hydrological and NWP Models, Phys. Chem. Earth (B), 25, 1221–1224, 2000.

Snyder, C. and Zhang, F.: Assimilation of Simulated Doppler Radar Observations with an Ensemble Kalman Filter, Mon. Wea. Rev., 131, 1663–1677, 2003.

Steppeler, J., Doms, G., Schättler, U., Bitzer, H.-W., Gassmann, A., Damrath, U., and Gregoric, G.: Meso-gamma Scale Forecasts using the Nonhydrostatic Model LM, Meteorol. Atmos. Phys., 82, 75–96, 2003.

Sun, J. and Crook, N. A.: Dynamical and Microphysical Retrieval from Doppler Radar Observations Using a Cloud Model and its Adjoint. Part I: Model Development and Simulated Data Experiments, J. Atmos. Sci., 54, 1642–1661, 1997.

Weisman, M. L. and Klemp, J. B.: The Dependence of Numerically Simulated Convective Storms on Vertical Wind Shear and Buoyancy, Mon. Wea. Rev., 110, 504–520, 1982.